

MAJOR PAPER

Biomarkers Predictive of Distant Disease-free Survival Derived from Diffusion-weighted Imaging of Breast Cancer

Maya Honda^{1,2*}, Mami Iima^{1,3}, Masako Kataoka¹, Yasuhiro Fukushima⁴,
Rie Ota¹, Akane Ohashi⁵, Masakazu Toi⁶, and Yuji Nakamoto¹

Purpose: To investigate whether intravoxel incoherent motion (IVIM) and/or non-Gaussian diffusion parameters are associated with distant disease-free survival (DDFS) in patients with invasive breast cancer.

Methods: From May 2013 to March 2015, 101 patients (mean age 60.0, range 28–88) with invasive breast cancer were evaluated prospectively. IVIM parameters (flowing blood volume fraction [f_{IVIM}] and pseudodiffusion coefficient [D^*]) and non-Gaussian diffusion parameters (theoretical apparent diffusion coefficient [ADC] at a b value of 0 s/mm² [ADC₀] and kurtosis [K]) were estimated using a diffusion-weighted imaging series of 16 b values up to 2500 s/mm². Shifted ADC values (sADC_{200–1500}) and standard ADC values (ADC_{0–800}) were also calculated. The Kaplan–Meier method was used to generate survival analyses for DDFS, which were compared using the log-rank test. Univariable Cox proportional hazards models were used to assess any associations between each parameter and distant metastasis-free survival.

Results: The median observation period was 80 months (range, 35–92 months). Among the 101 patients, 12 (11.9%) developed distant metastasis, with a median time to metastasis of 79 months (range, 10–92 months). Kaplan–Meier analysis showed that DDFS was significantly shorter in patients with $K > 0.98$ than in those with $K \leq 0.98$ ($P = 0.04$). Cox regression analysis showed a marginal statistical association between K and distant metastasis-free survival ($P = 0.05$).

Conclusion: Non-Gaussian diffusion may be associated with prognosis in invasive breast cancer. A higher K may be a marker to help identify patients at an elevated risk of distant metastasis, which could guide subsequent treatment.

Keywords: breast neoplasms, diffusion-weighted magnetic resonance imaging, intravoxel incoherent motion, kurtosis, prognosis

¹Department of Diagnostic Imaging and Nuclear Medicine, Kyoto University Graduate School of Medicine, Kyoto, Kyoto, Japan

²Department of Diagnostic Radiology, Kansai Electric Power Hospital, Osaka, Osaka, Japan

³Institute for Advancement of Clinical and Translational Science (iACT), Kyoto University Hospital, Kyoto, Kyoto, Japan

⁴Department of Applied Medical Imaging, Gunma University Graduate School of Medicine, Maebashi, Gunma, Japan

⁵Department of Translational Medicine, Diagnostic Radiology, Lund University, Skåne University Hospital, Malmö, Sweden

⁶Department of Breast Surgery, Kyoto University Graduate School of Medicine, Kyoto, Kyoto, Japan

*Corresponding author: Department of Diagnostic Imaging and Nuclear Medicine, Kyoto University Graduate School of Medicine, 54, Shogoinkawahara-cho, Sakyo-ku, Kyoto, Kyoto 606-8507, Japan. Phone: +81-75-751-3760, E-mail: mayah.217@gmail.com



This work is licensed under a Creative Commons Attribution-NonCommercial-NoDerivatives International License.

©2022 Japanese Society for Magnetic Resonance in Medicine

Received: May 4, 2022 | Accepted: June 12, 2022

Introduction

Breast cancer is a very common cancer in women, affecting 2.3 million new cases per year worldwide, and is a major cause of cancer deaths.¹ Metastases are responsible for as much as 90% of breast cancer deaths.^{2,3} Patients without detectable distant metastasis at the time of diagnosis may harbor undetectable micrometastases.⁴ Based on the rate of cancer progression and histopathological findings, patients with high-risk features can receive systemic chemotherapy and/or endocrine therapy to eradicate such occult disease. Several clinical and histopathological factors are known to be predictors of distant metastasis,^{5,6} but there is a room for improvement. Some researchers have focused on identifying imaging markers that can help predict distant metastasis using contrast-enhanced MRI.^{7–9}

The clinical use of diffusion-weighted imaging (DWI) has expanded and is now incorporated into routine clinical MRI protocol in many centers. The appeal of DWI is that it does

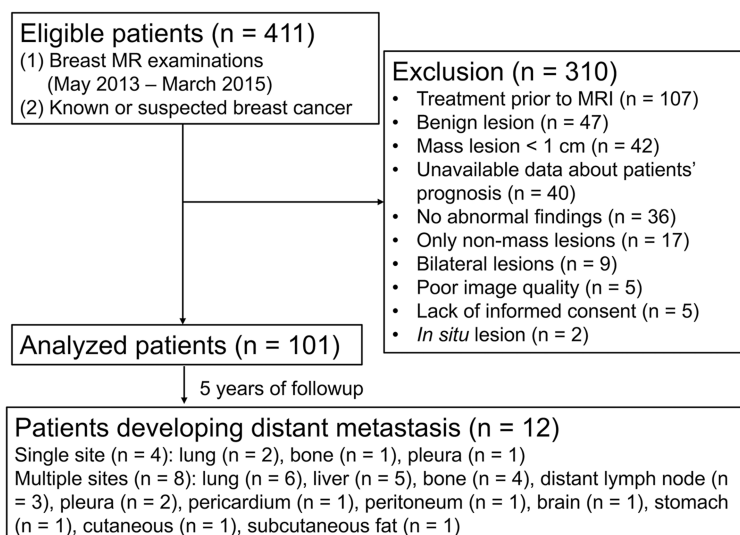


Fig. 1 Flowchart of patient selection and exclusion.

not require intravenous contrast to perform noninvasive and qualitative assessment of the biological characteristics of tumors. The apparent diffusion coefficient (ADC) is a robust parameter that is easy to derive from DWI. There is accumulating evidence of ADC's value in detection, diagnosis, and characterization of breast cancers, as well as prediction of treatment response.^{10,11} Recently, Kim et al. found that a wider range in ADC values within a tumor, reflecting intratumoral heterogeneity, was significantly and positively associated with the risk of distant metastasis.¹²

The ADC can be calculated from two b values (typically 0 and 800 s/mm²) but only weakly reflects non-Gaussian diffusion features in tissues.¹³ There are advanced techniques to better extract the non-Gaussian behavior of water diffusion and the intravoxel incoherent motion (IVIM) *in vivo*. IVIM effects are observed at low b values and include tissue diffusivity, as well as tissue microcapillary perfusion, observed as a pseudodiffusion process in the quasi-random organization in the space of capillary beds.¹⁴ Non-Gaussian DWI estimates the extent of kurtosis of water diffusion *in vivo* at high b-values. Since the deviation from Gaussian behavior is governed by the complexity of the tissue within which the water is diffusing, non-Gaussian diffusion effects can be regarded as a marker of tissue microstructures.¹⁵ Previous studies have revealed the utility of IVIM and non-Gaussian effects for discriminating malignant from benign breast lesions and association with subtypes or prognostic factors, such as the Ki-67 index and histologic grades.^{10,11} Shifted ADC (sADC) was conceived to shorten the acquisition time, which is calculated using only two shifted key b values optimized to differentiate tissue types from Gaussian and non-Gaussian diffusion altogether.¹⁶

To the best of our knowledge, the use of IVIM and non-Gaussian DWI to estimate the risk of distant metastasis has

not been investigated. The purpose of this study was to investigate whether these DWI parameters can predict distant metastasis-free survival in patients with invasive breast cancer.

Materials and Methods

Patients

This prospective study was approved by our institutional review board. From May 2013 to March 2015, 411 consecutive breast MR examinations were performed in patients with known or suspected breast cancer. Of the 411 patients, 310 patients were excluded according to the inclusion and exclusion criteria (Fig. 1), and the remaining 101 patients (mean age 60.0, range 28–88) were included in the study. There were 34.7% (35/101) cases of luminal A cancer, 11.9% (12/101) cases of luminal B/human epidermal growth factor 2 (HER2) positive cancer, 35.6% (36/101) cases of luminal B/HER2 negative cancer, 10.9% (11/101) cases of hormone receptor negative/HER2 positive cancer, and 6.9% (7/101) cases of triple negative cancer. Detailed patient characteristics according to distant metastasis pattern are shown in Table 1. When more than one mass was present, only the largest mass was considered so that the analysis would be performed on a per-patient basis. There are some patient data overlap with a previous study that analyzed lesion characterization in 199 breast cancer patients in 2018.¹⁷ The current study focused solely on patients' prognoses.

DWI acquisition

All images were acquired using a 3 T MRI scanner (Tim Trio; Siemens Healthineers, Erlangen, Germany) with a 16-channel dedicated breast coil. DWI data were acquired using a single-shot echo-planar imaging

Table 1 Patients' characteristics according to distant metastasis status

	Patient without distant metastasis (n = 89)	Patient with distant metastasis (n = 12)	P value ³
Age ¹	62.0 (50.0, 69.0)	50.5 (40.2, 71.8)	0.3
Tumor size ²			0.12
< 50 mm	50 (56%)	10 (83%)	
≥ 50 mm	39 (44%)	2 (17%)	
Neoadjuvant chemotherapy			0.2
No	57 (64%)	5 (42%)	
Yes	32 (36%)	7 (58%)	
Axillary node metastasis			0.11
Negative	60 (67%)	5 (42%)	
Positive	29 (33%)	7 (58%)	
Postoperative radiotherapy			0.8
No	40 (45%)	6 (50%)	
Yes	49 (55%)	6 (50%)	
Adjuvant chemotherapy			0.2
No	54 (61%)	5 (42%)	
Yes	35 (39%)	7 (58%)	
Anti-HER2 therapy			0.12
No	73 (82%)	7 (58%)	
Yes	16 (18%)	5 (42%)	
Adjuvant endocrine therapy			> 0.9
No	21 (24%)	3 (25%)	
Yes	68 (76%)	9 (75%)	
Estrogen receptor			0.7
Negative	15 (17%)	1 (8.3%)	
Positive	74 (83%)	11 (92%)	
Progesterone receptor			0.7
Negative	21 (24%)	2 (17%)	
Positive	68 (76%)	10 (83%)	
HER2 receptor			> 0.9
Negative	69 (78%)	9 (75%)	
Positive	20 (22%)	3 (25%)	
Ki-67 status ⁴			0.12
Negative	38 (43%)	2 (17%)	
Positive	51 (57%)	10 (83%)	

¹Data are median, with interquartile range in parentheses. ²Clinical tumor size based on ultrasonography and/or contrast-enhanced MRI. ³Wilcoxon rank-sum test; Fisher's exact test. ⁴Negative < 14%, Positive ≥ 14%. HER2, human epidermal growth factor 2.

prototype sequence with spectral attenuated inversion recovery for fat suppression; b values of 0, 5, 10, 20, 30, 50, 70, 100, 200, 400, 600, 800, 1000, 1500, 2000, and 2500 s/mm²; TR/TE, 4600/86 ms; FOV, 160 × 300 mm²; 80 × 166 matrix; section thickness, 3.0 mm; acquisition time, 3 min 55 s; generalized autocalibrating partially parallel acquisition (GRAPPA); and acceleration factor = 2.

Image analysis

Two independent radiologists (M.I., reader 1, with 9 years of experience in breast MRI and M.K., reader 2, with 19 years of experience in breast MRI) manually drew ROIs around each tumor from the b = 0 and b = 1000 s/mm² DW images using one slice with the largest cross-sectional area of the lesion. Care was taken to avoid necrotic or cystic areas exhibiting T2 shine-through. Diffusion parameters were estimated from means calculated from the ROIs. The estimation method was implemented with commercial software (MATLAB; Mathworks, Natick MA, USA) to run the analysis at the ROI level. These values were also calculated on a voxel-by-voxel basis and visualized on parametric maps. The image analysis was performed according to the previous study.¹⁷ Mean values from the two radiologists were calculated as the final results.

Estimation of IVIM and non-Gaussian diffusion parameters

The IVIM-derived pseudodiffusion coefficient (D*) and non-Gaussian-derived flowing blood volume fraction (f_{IVIM}), ADC₀, and kurtosis (K) were estimated using the kurtosis model with a two-step approach,¹⁸ first fitting the data for high b values (above 200 s/mm²) with the diffusion model,

$$S(b > 200) = \{S_0 \exp(-b^*ADC_0 + K[b^*ADC_0]^2/6) + NCF\}^{1/2} \quad (1)$$

where S₀ = theoretical signal acquired at b = 0 s/mm² and NCF = noise correction factor.

And then, the remaining signal was fitted after removing the diffusion component at low b values with the IVIM model to obtain estimates of f_{IVIM} and the pseudodiffusion, D*,

$$S_{IVIM} = S_{0IVIM} \exp(-bD^*) \quad (2)$$

$$f_{IVIM} = S_{0IVIM} / (S_{0IVIM} + S_{0DIFF}) \quad (3)$$

where S_{IVIM} is the raw signal intensity after the diffusion component has been removed and S_{0IVIM} is the theoretical signal from IVIM at b = 0 s/mm².

Standard ADC was calculated using b values of 0 and 800 s/mm² (ADC₀₋₈₀₀).

sADC, which encompasses both Gaussian and non-Gaussian effects, was calculated using b values of 200 and 1500 s/mm² (sADC_{200–1500}).

$$sADC = \ln \left\{ \frac{S_{LowKeyb}/S_{HighKeyb}}{LowKeyb - HighKeyb} \right\}, \quad (4)$$

where LowKeyb = 200 s/mm² and HighKeyb = 1500 s/mm².

Statistical analysis

Distant disease-free survival (DDFS) was defined as the period from the MR examination to the first occurrence of diagnosed distant metastasis. Distant metastasis was defined as the recurrence of breast cancer at a site other than the postoperative chest wall and regional lymph nodes, as confirmed by radiological and/or pathologic examinations. Data from patients who were lost to follow-up or had not developed distant metastasis at the last visit were treated as censored observations in this analysis. The final data collection took place on April 10, 2021, resulting in 6–8 years of follow-up.

The clinical-pathologic factors and quantitative DWI parameters were compared between patients with and without distant metastasis. Categorical variables were compared using the Fisher's exact test; continuous variables were compared using the Wilcoxon rank-sum test.

Survival analyses were performed for DDFS using the Kaplan–Meier method and were compared using the log-rank test. Univariable Cox proportional hazards models were used to assess the effects of each parameter on DDFS.

The interobserver variability between the radiologists for the f_{IVIM} , ADC₀, K, ADC_{0–800}, and sADC_{200–1500} values was evaluated by calculating intraclass correlation coefficients. For all tests, a *P* value < 0.05 was considered statistically significant. All statistical analyses were performed using open-source software (R-4.0.4; R Foundation for Statistical Computing, Vienna, Austria). The optimal cutoff values were calculated using the maxstat package of R.

Results

The median observation period was 80 months (range, 35–92 months). Among the 101 patients, 12 (11.9%) developed distant metastasis, with a median time to metastasis of 79 months (range, 10–92 months). A total of four patients had a single-site metastasis to the lung (*n* = 2), bone (*n* = 1), or pleura (*n* = 1). The remaining eight patients had multiple-site metastases with the following distribution: lung (*n* = 6), liver (*n* = 5), bone (*n* = 4), distant lymph node (*n* = 3), pleura (*n* = 2), pericardium (*n* = 1), peritoneum (*n* = 1), brain (*n* = 1), stomach (*n* = 1), cutaneous (*n* = 1), and subcutaneous fat (*n* = 1) (Fig 1). Three patients (3%) died of breast cancer during the observation period.

There were no DWI-derived parameters that showed statistically significant differences between patients with and without distant metastasis (Table 2).

Kaplan–Meier survival analysis showed that DDFS was significantly shorter in patients with higher K (> 0.98) than those with lower K (≤ 0.98, *P* = 0.04) (Fig 2). Cox regression analysis showed marginal statistical association between K and DDFS (*P* = 0.05). The same trend was evident in the results of each reader. The other parameters, including ADC₀, D*, f_{IVIM} , ADC_{0–800}, and sADC_{200–1500}, did not show statistical significance in Kaplan–Meier survival analysis.

Representative non-Gaussian DWI parameter maps are shown in Figs. 3 and 4. These parameter maps allow qualitative assessments of DWI parameters and visualization of the presence or absence of possible cancer metastasis.

The interobserver correlation between readers 1 and 2 was excellent for ADC₀ (*r* = 0.90), good for ADC_{0–800} and sADC_{200–1500} (*r* = 0.87 and 0.84, respectively), moderate for K (*r* = 0.65), and weak for f_{IVIM} (*r* = 0.27).

Discussion

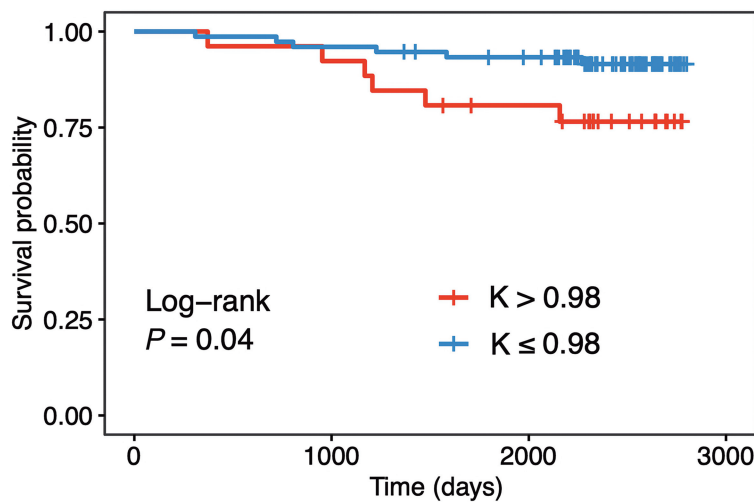
To the best of our knowledge, this study is the first to describe the ability of IVIM and non-Gaussian DWI parameters to predict distant metastasis in breast cancer patients. The current results suggest that K values can be useful prognostic indicators for distant metastasis from breast cancer, suggesting that non-Gaussian diffusion may be associated with prognosis. This will finally lead to personalized treatment options solely from MR acquisitions.

K is a kurtosis parameter representing a deviation from Gaussian diffusion, which may be related to the degree of microstructural complexity. Many studies have shown that malignant breast tumors have higher K values than benign tumors and that invasive cancers exhibit higher K values compared with *in situ* cancers,^{17–26} which might reflect the extent of water diffusion restriction due to microscopic features such as transmembrane ion transport in cancer cells.²⁷ In addition, some studies have demonstrated the positive correlation of K with histologic grades and Ki-67 expression.^{19,21} Huang et al. showed that a significantly higher K was observed in breast tumors with nodal involvement than in those without.²¹ As histologic grades and lymph node status are established prognostic indicators for breast cancer,^{6,28,29} it is not surprising that K can be an indicator of distant metastasis. It has also been reported that higher K values are associated with higher recurrence scores by the 21-gene recurrence score assay,³⁰ which quantifies the likelihood of 10-year distant recurrence in women with estrogen receptor-positive, lymph node-negative breast cancer treated with adjuvant tamoxifen.³¹ The 50th percentile of K from histogram analysis correlated with some of the 21 genes

Table 2 DWI-derived parameters according to distant metastatic status

Parameters	Overall (n = 101) ¹	Patients without distant metastasis (n = 89) ¹	Patients with distant metastasis (n = 12) ¹	P value ²
ADC ₀ (mm ² /s)	0.0011 ± 0.0004	0.0011 ± 0.0004	0.0010 ± 0.0004	0.3
K	0.8141 ± 0.2373	0.8011 ± 0.2400	0.9105 ± 0.1996	0.13
D*	0.0436 ± 0.1478	0.0462 ± 0.1571	0.0244 ± 0.0280	0.4
f _{IVIM}	0.0563 ± 0.0362	0.0585 ± 0.0372	0.0404 ± 0.0230	0.09
ADC _{200–1500} (mm ² /s)	0.0008 ± 0.0002	0.0008 ± 0.0002	0.0007 ± 0.0002	0.3
ADC _{0–800} (mm ² /s)	0.0010 ± 0.0003	0.0010 ± 0.0003	0.0009 ± 0.0002	0.2

¹Mean values with standard deviation are shown. ²Wilcoxon rank-sum test. ADC₀, diffusion coefficient at a b value of 0 s/mm²; DWI, diffusion-weighted imaging; D*, pseudodiffusion coefficient; f_{IVIM}, flowing blood volume fraction; K, kurtosis.



K	Number at risk by time			
> 0.98	26	24	19	0
≤ 0.98	75	72	66	0

Fig. 2 Kaplan–Meier plots of K. The distant metastasis-free survival times were significantly shorter in patients with higher K (> 0.98) than those with lower K (≤ 0.98, P = 0.04). K, kurtosis.

whose expression was evaluated in the same study, which means that K could be used to predict estrogen receptor-positive breast cancer recurrences.

The current results showed that ADC_{0–800} values did not correlate with distant metastasis-free survival times. A recent study by Kim et al. demonstrated that shorter distant metastasis-free survival times were associated with a higher ADC difference value, calculated as the difference between the minimum and maximum ADCs, and that mean ADC was not associated with the risk of distant metastasis as also seen in our study.¹² The authors speculated that the ADC difference value might better reflect intratumoral heterogeneity, which is positively associated with the risk of distant metastasis. One difference between the studies in terms of study

cohort is that our cohort included 34.7% luminal A breast cancer patients, which is closer to the proportion in the general population, while the cohort of the previous study included 28.7% luminal A breast cancer patients. The median follow-up period of this study was 80 months, longer than that of 51 months in the study by Kim et al.¹²

IVIM parameters did not affect the outcomes in our patient cohort. IVIM effect observed at low b values is known to carry information on the blood fraction, which may be associated with microperfusion and vascular density. Several studies have reported that IVIM parameters (especially D) have comparable diagnostic performance with ADC in distinguishing malignant from benign lesions in the breast, yet conflicting results have been reported on the

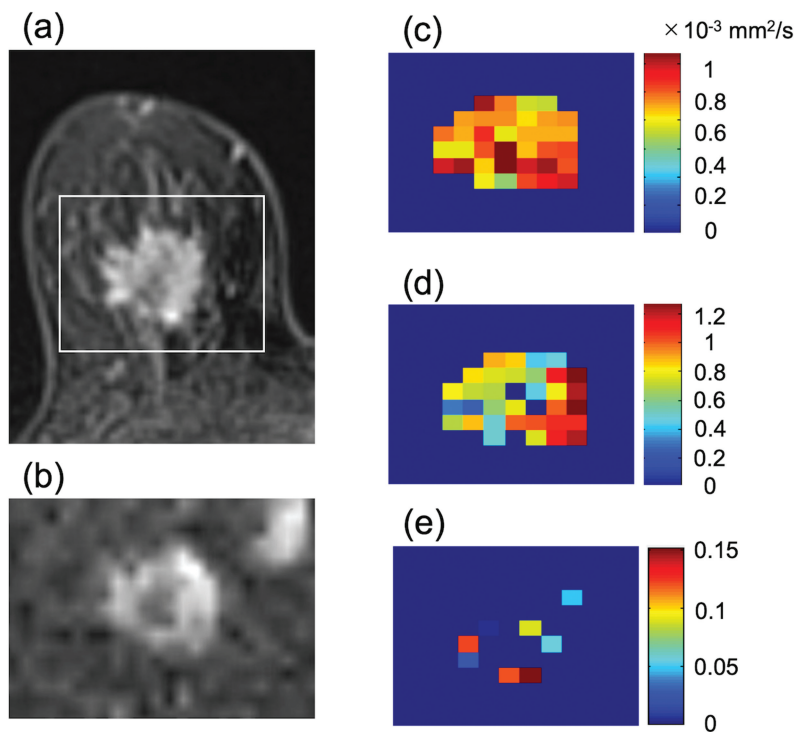


Fig. 3 Images of a 77-year-old woman with invasive ductal carcinoma who developed pleural metastasis 5 years and 11 months after MR examination. (a) contrast-enhanced axial MR image, (b) DWI ($b = 1500 \text{ s/mm}^2$), (c) ADC_0 map, (d) K map, (e) f_{IVIM} map. The white rectangle on (a) shows the area covered by the parametric maps. (a) The mass lesion is heterogeneously enhancing. (b) The lesion shows heterogeneously high signal intensity on DWI. (c) ADC_0 map shows low values throughout the lesion with a mean value of $0.9 \times 10^{-3} \text{ mm}^2/\text{s}$. (d) The mass shows relatively high mean K values (1.0) with heterogeneous distribution. (e) f_{IVIM} map shows low values throughout the lesion with a mean value of < 0.01 . ADC, apparent diffusion coefficient; DWI, diffusion-weighted imaging; f_{IVIM} , flowing blood volume fraction; K, kurtosis.

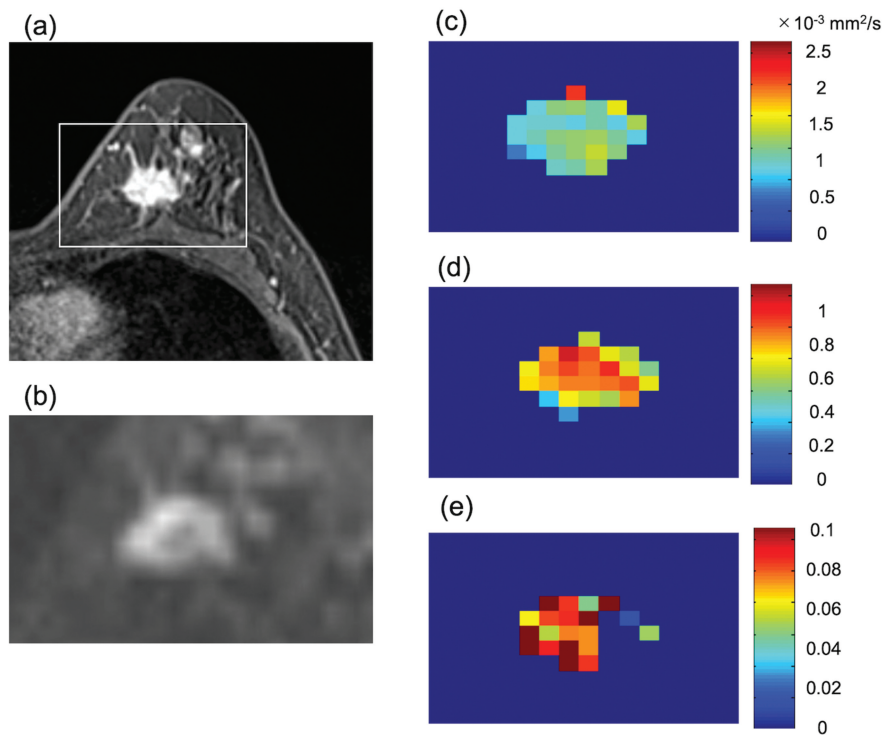


Fig. 4 Images of a 62-year-old woman with invasive ductal carcinoma who did not develop distant metastasis. (a) contrast-enhanced axial MR image, (b) DWI ($b = 1500 \text{ s/mm}^2$), (c) ADC_0 map, (d) K map, and (e) f_{IVIM} map. The white rectangle on (a) shows the area covered by the parametric maps. (a) The mass lesion showed heterogeneous enhancement. (b) The lesion shows peripheral high signal intensity on DWI. (c) ADC_0 map shows low values throughout the lesion with a mean value of $1.0 \times 10^{-3} \text{ mm}^2/\text{s}$. (d) The mass shows relatively low mean K values (0.83) with heterogeneous distribution. (e) f_{IVIM} map shows high values throughout the lesion with a mean value of 0.09. ADC, apparent diffusion coefficient; DWI, diffusion-weighted imaging; f_{IVIM} , flowing blood volume fraction; K, kurtosis.

association between IVIM parameters and prognostic factors.^{17,23,32} The current results suggest the inferiority of IVIM parameters in predicting distant metastasis compared to non-Gaussian diffusion parameters. The relatively low inter-observer agreement might also be an issue to be resolved in terms of IVIM parameters, not only for the breasts but also for other organs.³³ Still, IVIM is found to be useful for predicting prognosis for survival in patients with brain gliomas.³⁴ Some new IVIM models using Bayesian probability versus neural networks with good repeatability are also being explored, which might lead to a better estimation of IVIM values.³⁵

Tumor size and lymph node involvement, which are known to be major predictors of distant metastasis, did not show a significant difference between patients with and without distant metastasis in our results. The small sample size may have influenced this result, but another possibility is that the prognostic impact of these classic factors may be different from the past, due to recent advances in treatment. Detailed molecular profilings, such as Oncotype Dx (Genomic Health, Redwood City, CA, USA) and Mammaprint (Agendia, Irvine, CA, USA) breast cancer assays, molecular subclassification from whole-genome profiles, and, more recently, circulating tumor cell and cell-free deoxyribonucleic acid (DNA) assays, have been developed to identify patients at a high risk of recurrence or metastasis.⁴ Since MRI is a common imaging modality to evaluate breast cancer, MRI-derived imaging characteristics can be complementary markers to stratify the patients' risk of metastasis.

This study has some limitations. First, disease-free survival was not included in the analysis, as local recurrence is sometimes indistinguishable from a metachronous cancer. Second, overall survival was also not included because only three patients died in the cohort, which was too few for the analysis. Third, tumor heterogeneity was not considered in the ROI-based analysis of this study. Fourth, the treatment strategy was clinically determined based on the pathology and the physical and social factors of the patients. More than half of our patient cohort received neoadjuvant therapy. The choice of treatment may influence patient prognosis, and multivariate analysis including clinical and imaging factors with a larger patient cohort could be further investigated. Fifth, patients with small lesions were not included, so the study population may not be representative of patients with breast cancer in the general population, especially small lesions that might have a lower risk of metastasis. Sixth, the methods of patient follow-up intervals were inconsistent. Finally, the size of the cohort was small, and its distribution was somewhat skewed, so these preliminary results need to be confirmed from larger patient cohorts. There must be multiple imaging and clinical factors, including DWI parameters, that are associated with distant metastases, and a future large cohort study could elucidate these associations with multivariate analysis.

Conclusion

In summary, non-Gaussian diffusion may be associated with prognosis in breast cancer. Higher K before treatment may become an imaging marker to help identify patients with elevated risk of distant metastasis.

Acknowledgments

The authors thank Denis Le Bihan, MD, PhD, for his valuable advice to this study. We thank Libby Cone, MD, MA, from Effective Medical English (www.effectivemedicalenglish.com) for editing a draft of this manuscript.

Conflicts of Interest

Yasuhiro Fukushima has an endowed chair provided by Siemens Healthineers. The other authors declare no competing financial interests or personal relationships that could influence the work reported in this paper.

References

1. Sung H, Ferlay J, Siegel RL, et al. Global cancer statistics 2020: GLOBOCAN estimates of incidence and mortality worldwide for 36 cancers in 185 countries. *CA Cancer J Clin* 2021; 71:209–249.
2. Chaffer CL, Weinberg RA. A perspective on cancer cell metastasis. *Science* 2011; 331:1559–1564.
3. Medeiros B, Allan AL. Molecular mechanisms of breast cancer metastasis to the lung: Clinical and experimental perspectives. *Int J Mol Sci* 2019; 20:2272.
4. Redig AJ, McAllister SS. Breast cancer as a systemic disease: a view of metastasis. *J Intern Med* 2013; 274:113–126.
5. Rosa Mendoza ES, Moreno E, Caguioa PB. Predictors of early distant metastasis in women with breast cancer. *J Cancer Res Clin Oncol* 2013; 139:645–652.
6. Page DL. Prognosis and breast cancer. Recognition of lethal and favorable prognostic types. *Am J Surg Pathol* 1991; 15:334–349.
7. Zhao R, Ma WJ, Tang J, et al. Heterogeneity of enhancement kinetics in dynamic contrast-enhanced MRI and implication of distant metastasis in invasive breast cancer. *Clin Radiol* 2020; 75:961.e25–961.e32.
8. Ma W, Wang X, Xu G, et al. Distant metastasis prediction via a multi-feature fusion model in breast cancer. *Aging (Albany NY)* 2020; 12:18151–18162.
9. Song SE, Shin SU, Moon H-G, Ryu HS, Kim K, Moon WK. MR imaging features associated with distant metastasis-free survival of patients with invasive breast cancer: a case-control study. *Breast Cancer Res Treat* 2017; 162:559–569.
10. Iima M, Honda M, Sigmund EE, Ohno Kishimoto A, Kataoka M, Togashi K. Diffusion MRI of the breast: Current status and future directions. *J Magn Reson Imaging* 2020; 52:70–90.
11. Partridge SC, Nissan N, Rahbar H, Kitsch AE, Sigmund EE. Diffusion-weighted breast MRI: Clinical applications and emerging techniques. *J Magn Reson Imaging* 2017; 45:337–355.

12. Kim JY, Kim JJ, Hwangbo L, Kang T, Park H. Diffusion-weighted imaging of invasive breast cancer: Relationship to distant metastasis-free survival. *Radiology* 2019; 291:300–307.
13. Le Bihan D. Apparent diffusion coefficient and beyond: what diffusion MR imaging can tell us about tissue structure. *Radiology* 2013; 268:318–322.
14. Le Bihan D, Breton E, Lallemand D, Aubin ML, Vignaud J, Laval-Jeantet M. Separation of diffusion and perfusion in intravoxel incoherent motion MR imaging. *Radiology* 1988; 168:497–505.
15. Jensen JH, Helpert JA, Ramani A, Lu H, Kaczynski K. Diffusional kurtosis imaging: the quantification of non-gaussian water diffusion by means of magnetic resonance imaging. *Magn Reson Med* 2005; 53:1432–1440.
16. Iima M, Le Bihan D. Clinical intravoxel incoherent motion and diffusion MR imaging: Past, present, and future. *Radiology* 2016; 278:13–32.
17. Iima M, Kataoka M, Kanao S, et al. Intravoxel incoherent motion and quantitative non-gaussian diffusion MR imaging: Evaluation of the diagnostic and prognostic value of several markers of malignant and benign breast lesions. *Radiology* 2018; 287:432–441.
18. Iima M, Yano K, Kataoka M, et al. Quantitative non-Gaussian diffusion and intravoxel incoherent motion magnetic resonance imaging: differentiation of malignant and benign breast lesions. *Invest Radiol* 2015; 50:205–211.
19. Sun K, Chen X, Chai W, et al. Breast cancer: Diffusion kurtosis mr imaging-diagnostic accuracy and correlation with clinical-pathologic factors. *Radiology* 2015; 277:46–55.
20. Wu D, Li G, Zhang J, Chang S, Hu J, Dai Y. Characterization of breast tumors using diffusion kurtosis imaging (DKI). *PLoS One* 2014; 9: e113240.
21. Huang Y, Lin Y, Hu W, et al. Diffusion kurtosis at 3.0T as an in vivo imaging marker for breast cancer characterization: Correlation with prognostic factors. *J Magn Reson Imaging* 2019; 49:845–856.
22. Yang ZL, Li Y, Zhan CA, et al. Evaluation of suspicious breast lesions with diffusion kurtosis MR imaging and connection with prognostic factors. *Eur J Radiol* 2021; 145:110014.
23. Suo S, Cheng F, Cao M, et al. Multiparametric diffusion-weighted imaging in breast lesions: Association with pathologic diagnosis and prognostic factors. *J Magn Reson Imaging* 2017; 46:740–750.
24. Borlinhas F, Conceição RC, Ferreira HA. Optimal b-values for diffusion kurtosis imaging in invasive ductal carcinoma versus ductal carcinoma in situ breast lesions. *Australas Phys Eng Sci Med* 2019; 42:871–885.
25. Nogueira L, Brandão S, Matos E, et al. Application of the diffusion kurtosis model for the study of breast lesions. *Eur Radiol* 2014; 24:1197–1203.
26. Li Z, Li X, Peng C, et al. The diagnostic performance of diffusion kurtosis imaging in the characterization of breast tumors: A meta-analysis. *Front Oncol* 2020; 10:575272.
27. Springer CS Jr. Using $^1\text{H}_2\text{O}$ MR to measure and map sodium pump activity in vivo. *J Magn Reson* 2018; 291:110–126.
28. Soerjomataram I, Louwman MWJ, Ribot JG, Roukema JA, Coebergh JWW. An overview of prognostic factors for long-term survivors of breast cancer. *Breast Cancer Res Treat* 2008; 107:309–330.
29. Hayes DF, Isaacs C, Stearns V. Prognostic factors in breast cancer: current and new predictors of metastasis. *J Mammary Gland Biol Neoplasia* 2001; 6:375–392.
30. Wu J, Yan F, Chai W, et al. Breast cancer recurrence risk prediction using whole-lesion histogram analysis with diffusion kurtosis imaging. *Clin Radiol* 2020; 75:239.e1–239.e8.
31. Paik S, Tang G, Shak S, et al. Gene expression and benefit of chemotherapy in women with node-negative, estrogen receptor-positive breast cancer. *J Clin Oncol* 2006; 24:3726–3734.
32. Cho GY, Moy L, Kim SG, et al. Evaluation of breast cancer using intravoxel incoherent motion (IVIM) histogram analysis: comparison with malignant status, histological subtype, and molecular prognostic factors. *Eur Radiol* 2016; 26:2547–2558.
33. Iima M. Perfusion-driven intravoxel incoherent motion (IVIM) MRI in oncology: Applications, challenges, and future trends. *Magn Reson Med Sci* 2021; 20:125–138.
34. Federau C, Cerny M, Roux M, et al. IVIM perfusion fraction is prognostic for survival in brain glioma. *Clin Neuroradiol* 2017; 27:485–492.
35. Koopman T, Martens R, Gurney-Champion OJ, et al. Repeatability of IVIM biomarkers from diffusion-weighted MRI in head and neck: Bayesian probability versus neural network. *Magn Reson Med* 2021; 85:3394–3402.